Immunolocalization of endomucin-reactive blood vessels and α-smooth muscle actin-positive cells in murine nasal conchae

Haruhi Maruoka[1*], Tomoka Hasegawa[1§*], Hirona Yoshino[1], Miki Abe[1], Mai Haraguchi-Kitakamae[1, 4], Tomomaya Yamamoto[1, 5], Hiromi Hongo[1], Ko Nakanishi[2], Alireza Nasoori[1], Yuhi Nakajima[1], Masayuki Omaki[1], Yoshiaki Sato[3], Paulo Henrique Luiz de Fraitas[6], Minqi Li[7]

[1]Developmental Biology of Hard Tissue, [2]Biomaterials and Bioengineering, [3]Orthodontics, Graduate School of Dental Medicine and Faculty of Dental Medicine, Hokkaido University, Sapporo, Japan; [4]Division of Craniofacial Development and Tissue Biology, Graduate School of Dentistry, Tohoku University, Sendai, Japan; [5]Northern Army Medical Unit, Camp Makomanai, Japan Ground Self-Defense Forces, Sapporo, Japan; [6]Department of Dentistry, Federal University of Sergipe, Lagarto, SE, Brazil; [7]Shandong Provincial Key Laboratory of Oral Biomedicine, The School of Stomatology, Shandong University, Jinan, China

*These authors equally contributed to this work.

Running title: ***endomucin and αSMA in nasal conchae***

[§]Corresponding Author:

Tomoka Hasegawa, D.D.S., Ph.D.
Developmental Biology of Hard Tissue
Graduate School of Dental Medicine
Faculty of Dental Medicine, Hokkaido University
Kita 13, Nishi 7, Kita-Ku, Sapporo, Hokkaido 060-8586, Japan
Tel/Fax: +81-11-706-4226
E-mail: hasegawa@den.hokudai.ac.jp

ABSTRACT

Objectives: Recently, the biological functions of endomucin-positive blood vessels and closely associated αSMA-positive cells in long bones have been highlighted. The surrounding tissues of the flat bones, such as nasal bones covered with mucosa and lamina propria, are different from those of the long bones, indicating the different distributions of endomucin-positive blood vessels and αSMA-reactive cells in nasal bones. This study demonstrates the immunolocalization of endomucin-reactive blood vessels and αSMA-positive cells in the nasal conchae of 3- and 7-week-old mice.

Methods: The nasal conchae of 3-week-old and 7-week-old male C57BL/6J mice were used for immunoreaction of endomucin, CD34, PDGFbb, TRAP, and c-kit.

Results: While we identified abundant endomucin-reactive blood vessels in the lamina propria neighboring the bone, not all were positive for endomucin. More CD34-reactive cells and small blood vessels were observed in the nasal conchae of 3-week-old mice than in those of 7-week-old mice. Some αSMA-positive cells in the nasal conchae surrounded the blood vessels, indicating vascular smooth muscle cells, while other αSMA-immunopositive fibroblastic cells were detected throughout the lamina propria. αSMA-positive cells did not co-localize with C-kit-immunoreactivity, thereby indicating that the αSMA-positive cells may be myofibroblasts rather than undifferentiated mesenchymal cells.

Conclusions: Unlike long bones, nasal conchae contain endomucin-positive as well as endomucin-negative blood vessels and exhibit numerous αSMA-positive fibroblastic cells throughout the lamina propria neighboring the bone. Apparently, the distribution patterns of endomucin-positive blood vessels and αSMA-positive cells in nasal conchae are different from those in long bones.

241 words

Key words: *nasal bone, blood vessel, endomucin, alpha smooth muscle actin*

1. Introduction

The nasal conchae—scroll-shaped, flattened bones that protrude into the nasal cavity—are covered by mucosa, such as the stratified epithelium of the nasal vestibule, the respiratory epithelium covering most of the cavity, and the olfactory epithelium covering the posterodorsal part of the septum. The lamina propria beneath the epithelial layers tightly connects to the bones of the conchae. The trabeculae of the cancellous bones of the femora and tibiae, unlike the bones of the nasal conchae, are surrounded by bone marrow tissue.

The cancellous bones of the femora and tibiae are rich in blood vessels including sinusoids. The subtypes of bone-specific endothelial cells that are found in long bones have been reported to be strongly positive for both CD31 and endomucin [1, 2], the latter of which is a mucin-like sialoglycoprotein with a molecular weight of 80–120 kDa that is endothelial-specific and expressed solely on the capillary and venous, but not the arterial, endothelium [3–6]. Endomucin-positive bone-specific blood vessels reportedly interact with osteoblasts [1, 2], and the angiogenesis of blood vessels seems to be partially induced by platelet-derived growth factor (PDGF) bb secreted by osteoclasts [7]. A previous report demonstrated that vascular endothelial cells in arteries and arterioles express ephrinB2, whereas endothelial cells in veins contain EphB4 [8]. Based on the previous reports, we have recently presented evidence for a large number of EphB4-positive/endomucin-reactive blood vessels in the femoral metaphyses of mice [9].

The micro-environment surrounding the metaphyseal trabeculae very likely differs from that surrounding the blood vessels of the nasal conchae. Grevers and Herrmann have proposed a biological link between the morphological characteristics of the vascular wall of blood vessels and the functional behavior of the nasal mucosa, describing endothelial fenestrations as one of the characteristics of the microcirculatory system in the nasal mucosa [10]. The microcirculatory system in the nasal mucosa appears to play a major role in, for example, nasal allergy and reaction to cold exposure, and we therefore assumed differences between the physiological functions and the environment surrounding the blood vessels in the nasal conchae and the functions and environment of the metaphyseal cancellous bones of the femora and tibiae.

Regarding alpha smooth muscle actin (αSMA)-positive cells in the femora and tibiae, it is known that only few αSMA-positive vascular smooth muscle cells surround the endomucin-reactive blood vessels in a normal state. However, we have recently reported that parathyroid hormone (PTH) administration significantly increases the numbers of blood vessels surrounded

by αSMA-positive cells [11]. These αSMA-positive cells are not only smooth muscle cells surrounding the blood vessels, but also fibroblastic cells originating from the blood vessels and extending towards the bone cells. The blood vessel-derived αSMA-positive cells extending close to osteoblasts were found to be immunoreactive for c-kit, a type-III receptor tyrosine kinase that transduces signaling by binding stem cell factor [12], which is a hallmark of undifferentiated cells, as well as to tissue-nonspecific alkaline phosphatase (ALP, a marker of osteoblastic lineage). This suggests that αSMA-positive fibroblastic cells derived from blood vessels might be undifferentiated but somehow committed to an osteoblastic lineage. Thus, in a normal state, only a few blood vessels are surrounded by αSMA-positive vascular smooth muscle cells.

In contrast, only a few literatures have described αSMA-positive cells in the nasal conchae; fibroblasts in the nasal mucosa could reportedly transdifferentiate into αSMA-positive myofibroblasts [13]. Jacob *et al.* found that the multipotent mesenchymal stromal cells in the nasal mucosa have the potential to differentiate along the adipogenic, chondrogenic, and osteogenic pathways [14, 15]. Recently, a single-cell RNA sequencing analysis demonstrated that mesenchymal stem cells in the nasal conchae originate from a perivascular or pericyte population [16], which indicates that there are mesenchymal stem cells in the nasal mucosa. However, whether there is a significant number of αSMA-positive cells in the nasal conchae and whether these αSMA-positive cells could be undifferentiated mesenchymal cells is still unclear.

In addition, it is necessary to consider the growth of the murine heads including nasal regions. According to Wei *et al.*, it seems preferable to compare nasal conchae between 3-week-old mice, which show an increasing head length and 7-week-old mice, which have reached the beginning of the plateau of head growth even though their body weight is still increasing [17]. Based on these finding, this study aimed to examine the immunolocalization of αSMA-positive cells in association with endomucin-positive bone-specific blood vessels in the nasal conchae at the growing stage of heads (3-week-old mice) and at the beginning of the plateau of head growth (7-week-old mice).

2. Materials and Methods

2. 1. Animals and preparation of histochemical specimens

Nasal conchae of 3-week-old and 7-week-old male C57BL/6J mice (n=6 of each age group, Japan CLEA, Tokyo, Japan) were used in this study, which followed the principles for animal care and research use set by Hokkaido University where all experiments were conducted (approval no. #18-0076). Mice were anesthetized with an intraperitoneal injection of a mixture containing 0.3 mg/kg of medetomidine, 4.0 mg/kg of midazolam, and 5.0 mg/kg of butorphanol. All mice were then perfused with 4% paraformaldehyde diluted in 0.1 M phosphate buffer (pH 7.4) through the cardiac left ventricle. The heads were immediately removed and immersed in the same fixative for 24 h at 4 °C. The samples were decalcified with a solution of 10% ethylene diamine tetraacetic disodium salt and dehydrated in ascending ethanol solutions prior to paraffin embedding. The histological sections were made parallel to the assumed line of molars in maxillae prior to immunohistochemical examination.

2. 2. Single immunohistochemical studies

Paraffin-embedded histological sections were used for an immunohistochemical examination of the following antigens: endomucin, αSMA, and CD34. After deparaffinization, standardized procedures for immunostaining were followed as reported previously [18]. In brief, sections were treated for endogenous peroxidase inhibition with 0.3% H_2O_2 in PBS for 30 min, and subsequently for nonspecific stain blocking with 1% bovine serum albumin (BSA; Serologicals Proteins Inc. Kankakee, IL) in PBS (1% BSA-PBS) for 20 min at room temperature. After that, sections were incubated with the corresponding pair of antibodies according to the antigen of interest (primary/secondary), as follows: 1) endomucin, rat antibody against endomucin (Santa Cruz Biotechnology, Inc., Dallas, TX; diluted 1:100)/horseradish peroxidase (HRP)-conjugated anti-rat IgG (Zymed Laboratories Inc., South San Francisco, CA; diluted 1: 100); 2) αSMA, mouse antibody against αSMA (Thermo Fisher Scientific Inc., Cheshire, UK; diluted 1: 400)/HRP-conjugated anti-mouse IgG (Invitrogen Co., Camarillo, CA); 3) CD34, rabbit antibody against CD34 (Abcam plc., Cambridge, UK; diluted 1: 50)/HRP-conjugated anti-rabbit IgG (DakoCytomation, Glostrup, Denmark; diluted 1: 100). Immunoreactions were assessed using 3, 3'-diaminobenzidine tetrahydrochloride (Dojindo Laboratories, Kumamoto, Japan). Specimens were then observed under a Nikon Eclipse Ni microscope (Nikon Instruments Inc. Tokyo, Japan) and light microscopic images were acquired with a digital camera (Nikon DXM1200C, Nikon).

2.3. Double detection of PDGFbb/tartrate resistant acid phosphatase (TRAP) and

αSMA/ALP

For double detection of PDGFbb/TRAP, the dewaxed sections were reacted with mouse anti-PDGFbb (Abcam plc., diluted 1: 100) and then incubated with HRP-conjugated anti mouse IgG (Invitrogen, diluted 1:100). For TRAP detection, immunostained sections were immersed in an aqueous solution containing 2.5 mg of naphthol AS-BI phosphate (Sigma-Aldrich, St. Louis, MO) and 18 mg of Fast Blue RR salt (Sigma-Aldrich) diluted in 30 ml of a 0.1M Tris-HCl buffer (pH 8.5) for 15 min at 37 °C, until immunoreactivity was visible. For endomucin/αSMA double immunohistochemical staining, dewaxed paraffin sections were incubated with 1% BSA-PBS, then with mouse antibody against αSMA (Thermo Fisher), and subsequently with HRP-conjugated secondary antibody as described above. The immunoreacted sections were incubated with anti-endomucin antibody (Santa Cruz), followed by incubation with ALP-conjugated goat anti-rat IgG (Jackson Immuno Research Laboratories, Inc., West Grovw, PA). HRP and ALP visualization was conducted as described above.

2. 4. Double immunofluorescent detection of αSMA/c-kit

For immunofluorescent detection of αSMA/c-kit, dewaxed sections were incubated with mouse antibody against αSMA (Thermo Fisher) and then with Alexa488-conjugated anti-mouse IgG (Invitrogen, diluted 1: 100). Thus-treated sections were reacted with goat antibody against c-kit (R&D Systems Inc., Minneapolis, MN, diluted 1: 25) and then with Alexa 594-conjugated anti-goat IgG (Invitrogen, diluted 1: 100). All sections were embedded in VECTASHIELD hard-set mounting medium with DAPI (Vector Laboratories, Inc. Burlingame, CA).

2. 5. Calculation of numbers of total, endomucin-reactive, and CD34-positive blood vessels

Histological images of the nasal conchae were acquired with a digital camera with an X40 objective lens; three images of assumed boxed areas of 236 μm (width)×342 μm (length) in different regions were taken in each specimen immunostained with endomucin or CD34 (n=6 for each group of 3-week-old and 7-week-old mice). Mean values of the total numbers, endomucin-reactive, and CD34-positive blood vessels were calculated for each specimen using the three images, and the mean values for the six specimens from each age group were used for further analysis. The numbers of blood vessels were counted by three blinded volunteers.

2. 6. Statistical analysis

The statistical analyses were performed by using BellCurve for Excel (Social Survey Researcj

Information Co., Ltd.). All values are presented as median (lower quartile–upper quartile). Shapiro-Wilk test was used to determine the normality, and then the difference between the 3-week-old and 7-week-old mice was analyzed by the Mann-Whitney U test. Values of $P<0.05$ were considered statistically significant.

3. Results

3. 1. Distribution of endomucin-immunoreactive blood vessels in the nasal conchae

The nasal conchae showed immature bone characterized by fine trabeculae containing a high number of osteocytes at 3 weeks of age, while the bone profile observed at 7 weeks of age seemed relatively mature **(Fig. 1a–d)**. In both 3-week-old and 7-week-old mice, the thick lamina propria containing many blood vessels had developed between the epithelium and the bone **(Fig. 1e, f)**. Endomucin-immunopositive blood vessels were also observed in the lamina propria of the nasal conchae in both 3-week-old and 7-week-old mice **(Fig. 2a, b)**. However, not all blood vessels were immunopositive for endomucin; we detected a high number of endomucin-negative blood vessels in the nasal conchae of both 3-week-old and 7-week-old mice **(Fig. 2c, e)**. Statistical analysis showed no significant difference in the percentage of endomucin-positive blood vessels between the 3-week-old and 7-week-old mice **(Fig. 2g)**. Approximately 30–40% of blood vessels were positive for endomucin (34.704% [33.557–38.778%] vs 34.025% [30.086–38.961%], difference not significant, 3-week-old vs 7-week-old mice). In the lamina propria of the nasal conchae of 3-week-old and 7-week-old mice, we detected cells and small blood vessels that were positive for CD34—one of the hallmarks of endothelial progenitor cells **(Fig. 2d, f)** [19, 20]. The ratio of CD34-reactive to total numbers of blood vessels was significantly higher in 3-week-old mice than in 7-week-old mice (26.186% [24.516–27.348%] vs 13.798% [5.629–15.823%], $P<0.05$, 3-week-old vs 7-week-old mice) **(Fig. 2h)**. In the long bones, since osteoclasts reportedly synthesize PDGFbb, which indicates their close association with the angiogenesis of blood vessels in bone [7], we examined the double immunodetection of PDGFbb-reactive/TRAP-positive osteoclasts **(Fig. 3a–c)**. TRAP-reactive osteoclasts with PDGFbb-immunoreactivity were mostly localized to one side of the conchae bone but hardly seen on the other side **(Fig. 3d, e)**. Unexpectedly, endomucin-positive blood vessels were localized not only one side of the conchae with many TRAP-positive/PDGFbb-immunoreactive osteoclasts, but also observed in the other side of conchae

(Fig. 3f). This implies no spatial correlation in the distribution of PDGFbb-reactive/TRAP-positive osteoclasts and endomucin-positive blood vessels.

3. 2. Distribution of αSMA-immunoreactive cells in the nasal conchae

We next examined the immunolocalization of endomucin-positive blood vessels and αSMA-reactive cells in the conchae of both 3-week-old and 7-week-old mice **(Fig. 4a, b)**. Many αSMA-immunoreactive fibroblastic cells were observed throughout the lamina propria between the epithelium and the bone **(Fig. 4c–f)**. Some endomucin-reactive blood vessels were surrounded by αSMA-reactive vascular smooth muscle cells while others were not, in both 3-week-old and 7-week-old mice **(Fig. 4c, d)**. In the region of the thick lamina propria, many αSMA-positive fibroblastic cells extended their cytoplasmic processes, which indicates no close histological association of endomucin-positive blood vessels and αSMA-reactive cells **(Fig. 4e, f)**. To define if these αSMA-positive fibroblastic cells are undifferentiated mesenchyme cells as suggested by Jakob *et al.* [14, 15], we compared the immunolocalization of αSMA cells and cells positive for c-kit. Immunofluorescent analyses demonstrated the similar localization of αSMA-immunopositive cells and c-kit-reactive cells in the lamina propria in 3-week-old mice **(Fig. 5a–d)**. However, images at higher magnification revealed that αSMA-positive cells were in close proximity of, but not overlapping with, c-kit-immunopositive cells **(Fig. 5e, f)**.

4. Discussion

We have recently demonstrated that the metaphyses of the femora and tibiae exhibit many endomucin-positive blood vessels that are also immunoreactive for EphB4, with the exception of the region close to the chondro-osseous junction—a site of vascular invasion into the growth plate cartilage [9]. In contrast, in the current study, only 30–40% of all blood vessels in the nasal conchae showed endomucin-immunoreactivity, and the endomucin-reactive blood vessels did not show spatially close associations with PDGFbb-reactive/TRAP-positive osteoclasts. This implies that the blood vessels in the nasal conchae are not functionally similar to those in the metaphyses of long bones. We also observed an increase in the numbers of CD34-positive small blood vessels, which implies active angiogenesis in the nasal conchae at 3 rather than 7 weeks of age, which seems to be in line with the growth process of the nasal conchae.

Endomucin is an endothelial-specific, mucin-like sialoglycoprotein that is expressed solely on the capillary and venous, but not the arterial, endothelium [3–6]. The lamina propria of the nasal conchae contains not only veins and venules but also arterial endothelia, which do not show endomucin, thereby forming a microcirculation system specific to nasal circumstances. Endomucin reportedly inhibits the assembly of focal adhesion complexes and the interaction between cells and the extracellular matrix [21] as well as between neutrophils and endothelial cells [22]. On the other hand, the nasal conchae are often exposed to inflammatory circumstances, due to, for example, rhinitis and allergy, and to external stimulants such as mechanical force; the blood vessels in the nasal conchae may therefore be adapted to these stimuli, presumably by interacting with extracellular matrices as well as neutrophils and lymphocytes. Hence, the microcirculatory circumstances in the nasal mucosa seem to differ from those in the metaphyses of the femora and tibiae.

We have previously reported that we detected only few αSMA-positive blood vessels in normal metaphyses of the tibiae and femora [11]. After the administration of parathyroid hormone (PTH), a number of αSMA-positive blood vessels appeared, not only surrounding the blood vessels but also extending out of the periphery of the blood vessels, thus exhibiting a characteristic of undifferentiated cells while somehow being committed to an osteoblastic fate [11]. In the current study, in contrast to the long bones, many αSMA-positive fibroblastic cells were seen throughout the lamina propria of the nasal conchae of the 3-week-old and 7-week-old mice. Some reports have proposed that αSMA serves as a marker of undifferentiated mesenchymal cells [23–25], while others suggested that αSMA indicates fully-differentiated myofibroblasts [26, 27]. Since αSMA-positive fibroblastic cells were not co-localized with c-kit-reactive cells in our current examination, we assume that αSMA-positive fibroblastic cells might be myofibroblasts rather than undifferentiated mesenchyme cells. Myofibroblasts have been discovered in the periodontal ligaments of teeth, assumedly in response to mechanical force and to alter the microenvironment of the extracellular matrix [27]. αSMA-positive cells in the periodontal ligaments have the potential to trans-differentiate from periodontal fibroblasts into myofibroblasts, thereby playing a role in contractile activity against mechanical stress, e.g., occlusion [28]. Taken together, it is likely that the reason why the lamina propriae interconnecting the epithelium and bone contain many αSMA-positive myofibroblasts is that the nasal conchae are easy to undertake the mechnical force.

In contrast to αSMA-positive myofibroblasts, Suphanantachat *et al.* have demonstrated

an important role of c-kit in maintaining the undifferentiated stage of mesenchymal cells [12]. Since cells in the lamina propria of the nasal conchae can reportedly differentiate into osteogenic cells [29–31], it might be the c-kit-reactive cells, rather than the αSMA-positive cells, that undergo this differentiation under certain circumstances.

5. Conclusion

Although the lamina propria is closely connected to the bone of the nasal conchae, we found that unlike in the metaphyseal trabeculae of the femora and tibiae, 30–40% of blood vessels in this layer were positive for endomucin, indicating that veins and venules are not predominant in the nasal conchae in mice between the age of 3 and 7 weeks. Many αSMA-positive fibroblastic cells that did not exhibit c-kit immunoreactivity were present throughout the lamina propria, and the αSMA-positive fibroblastic cells did not only surround the blood vessels but also extended their cytoplasmic processes. This suggests that the αSMA-positive cells in the nasal conchae might be myofibroblasts, presumably responding to specific nasal physiological and pathological circumstances such as mechanical force and inflammation.

Ethical statement

The study followed the principles for animal care and research use set by Hokkaido University (approval no. #18-0076).

Funding

This study was partially supported by the Grants-in-Aid for Scientific Research program of the Japan Society for the Promotion of Science (funding awarded to Hasegawa T.).

Conflicts of interest

The authors declare no conflict of interest.

References

1. Kusumbe AP, Ramasamy SK and Adams RH. Coupling of angiogenesis and osteogenesis by a specific vessel subtype in bone. Nature 2014; 507: 323–328.

2. Ramasamy SK, Kusumbe AP, Wang L and Adams RH. Endothelial Notch activity promotes angiogenesis and osteogenesis in bone. Nature. 2014; 507: 376–380.

3. Morgan SM, Samulowitz U, Darley L, Simmons DL and Vestweber D. Biochemical characterization and molecular cloning of a novel endothelial-specific sialomucin. Blood. 1999; 93: 165–175.

4. Samulowitz U, Kuhn A, Brachtendorf G, Nawroth R, Braun A, Bankfalvi A et al. Human endomucin: distribution pattern, expression on high endothelial venules, and decoration with the MECA-79 epitope. Am J Pathol. 2002; 160: 1669–1681.

5. dela Paz NG and D'Amore PA. Arterial versus venous endothelial cells. Cell Tissue Res. 2009; 335: 5–16.

6. Zuercher J, Fritzsche M, Feil S, Mohn L and Berger W. Norrin stimulates cell proliferation in the superficial retinal vascular plexus and is pivotal for the recruitment of mural cells. Hum Mol Genet. 2012; 21: 2619–2630.

7. Xie H, Cui Z, Wang L, Xia Z, Hu Y, Xian L et al. PDGF-BB secreted by preosteoclasts induces angiogenesis during coupling with osteogenesis. Nat Med 2014; 20: 1270–1278.

8. Wang HU, Chen ZF and Anderson DJ. Molecular distinction and angiogenic interaction between embryonic arteries and veins revealed by ephrin-B2 and its receptor Eph-B4. Cell 1998; 93: 741–753.

9. Tsuchiya E, Hasegawa T, Hongo H, Yamamoto T, Abe M, Yoshida T et al. Histochemical assessment on the cellular interplay of vascular endothelial cells and septoclasts during endochondral ossification in mice. Microscopy (Oxf) 2021; 70: 201–214.

10. Grevers G and Herrmann U. Fenestrated endothelia in vessels of the nasal mucosa. An electron-microscopic study in the rabbit. Arch Otorhinolaryngol. 1987; 244: 55–60.

11. Zhao S, Hasegawa T, Hongo H, Yamamoto T, Abe M, Yoshida T et al. Intermittent PTH administration increases bone-specific blood vessels and surrounding stromal cells in murine long bones. Calcif Tissue Int. 2021; 108: 391–406.

12. Suphanantachat S, Iwata T, Ishihara J, Yamato M, Okano T and Izumi Y. A role for c-Kit in the maintenance of undifferentiated human mesenchymal stromal cells. Biomaterials. 2014; 35: 3618–3626.

13. Kumar V, Ali MJ and Ramachandran C. Effect of mitomycin-C on contraction and migration of human nasal mucosa fibroblasts: implications in dacryocystorhinostomy. Br J Ophthalmol. 2015; 99: 1295–1300.

14. Jakob M, Hemeda H, Janeschik S, Bootz F, Rotter N, Lang S et al. Human nasal mucosa contains tissue-resident immunologically responsive mesenchymal stromal cells. Stem Cells Dev. 2010; 19: 635–644.

15. Jakob M, Hemeda H, Bruderek K, H Gerstner AO, Bootz F, Lang S et al. Comparative functional cell biological analysis of mesenchymal stem cells of the head and neck region: potential impact on wound healing, trauma, and infection. Head Neck 2013; 35: 1621–1629.

16. Choi R, Goncalves S, Durante MA and Goldstein BJ. On the in vivo origin of human nasal mesenchymal stem cell cultures. Laryngoscope Investig Otolaryngol. 2020; 5: 975–982.

17. Wei X, Thomas N, Hatch NE, Hu M and Liu F. Postnatal Craniofacial Skeletal Development of Female C57BL/6NCrl Mice. Frontiers in Physiology 2017; 8: 697.

18. Hasegawa T, Yamamoto T, Sakai S, Miyamoto Y, Hongo H, Qiu Z et al. Histological effects of the combined administration of eldecalcitol and a parathyroid hormone in the metaphyseal trabeculae of ovariectomized rats. J Histochem Cytochem. 2019; 67: 169–184.

19. Asahara T, Murohara T, Sullivan A, Silver M, van der Zee R, Li T et al. Isolation of putative progenitor endothelial cells for angiogenesis. Science. 1977; 275: 964–967.

20. Hur J, Yoon CH, Kim HS, Choi JH, Kang HJ, Hwang KK et al. Characterization of two types of endothelial progenitor cells and their different contributions to neovasculogenesis. Arteriescler Throm Vas Biol. 2004; 24: 288–293.

21. Kinoshita M, Nakamura T, Ihara M, Haraguchi T, Hiraoka Y, Tashiro K et al. Identification of human endomucin-1 and -2 as membrane-bound O-sialoglycoproteins with anti-adhesive activity. FEBS Lett. 2001; 499: 121–126.

22. Zahr A, Alcaide P, Yang J, Jones A, Gregory M, dela Paz NG et al. Endomucin prevents leukocyte-endothelial cell adhesion and has a critical role under resting and inflammatory conditions. Nat Commun. 2016; 7: 10363.

23. Cai D, Marty-Roix R, Hsu HP and Spector M. Lapine and canine bone marrow stromal cells contain smooth muscle actin and contract a collagen-glycosaminoglycan matrix. Tissue Eng. 2001; 7: 829–841.

24. Kinner B, Zaleskas JM and Spector M. Regulation of smooth muscle actin expression and contraction in adult human mesenchymal stem cells. Exp Cell Res. 2002; 278: 72–83.

25. Yamada M, Kurihara H, Kinoshita K and Sakai T. Temporal expression of alpha-smooth muscle actin and drebrin in septal interstitial cells during alveolar maturation. J Histochem Cytochem. 2005; 53: 735–744.

26. Giannopoulou C and Cimasoni G. Functional characteristics of gingival and periodontal ligament fibroblasts. J Dent Res. 1996; 75: 895–902.

27. Xu H, Bai D, Ruest LB, Feng JQ, Guo YW, Tian Y et al. Expression analysis of a-smooth muscle actin and tenascin-C in the periodontal ligament under orthodontic loading or in vitro culture. Int J Oral Sci. 2015; 7: 232–241.

28. Dorotheou D, Bochaton-Piallat ML, Giannopoulou C and Kiliaridis S. Expression of a-smooth muscle actin in the periodontal ligament during post-emergent tooth eruption: J Int Med Res. 2018; 46: 2423–2435.

29. Delorme B, Nivet E, Gaillard J, Häupl T, Ringe J, Deveze A, et al. The human nose harbors a niche of olfactory ectomesenchymal stem cells displaying neurogenic and osteogenic properties. Stem Cells Dev. 2010; 19: 853–866.

30. Shafiee A, Kabiri M, Ahmadbeigi N, Yazdani SO, Mojtahed M, Amanpour S et al. Nasal septum-derived multipotent progenitors: a potent source for stem cell-based regenerative medicine. Stem Cells Dev. 2011; 20: 2077–2091.

31. Torreggiani E, Bianchini C, Penolazzi L, Lambertini E, Vecchiatini R et al. Osteogenic potential of cells derived from nasal septum. Rhinology. 2011; 49: 148–154.

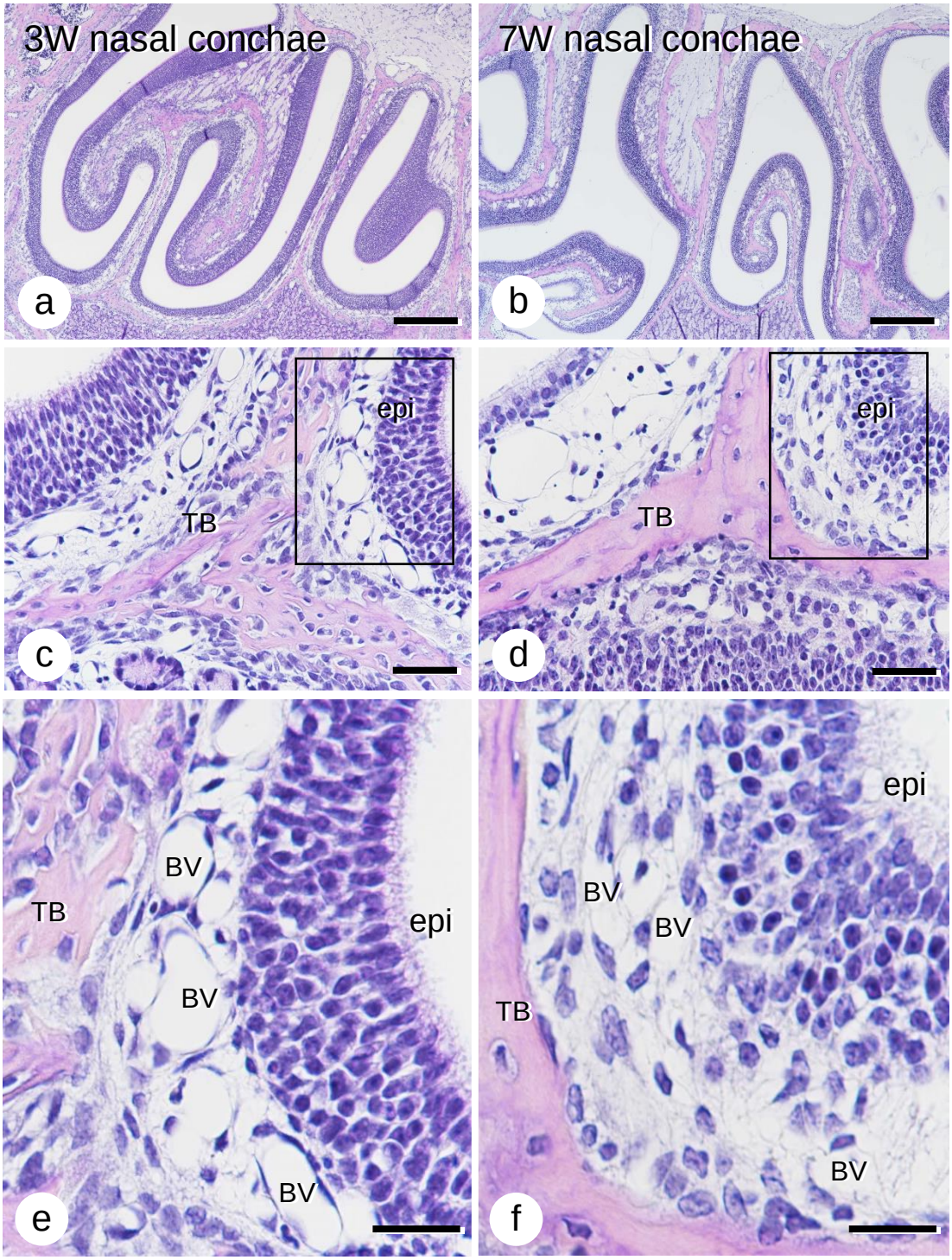
3W nasal conchae
a
7W nasal conchae
b
epi
TB
c
epi
TB
d
BV
TB
epi
BV
BV
e
epi
BV
BV
TB
BV
f

Fig.1

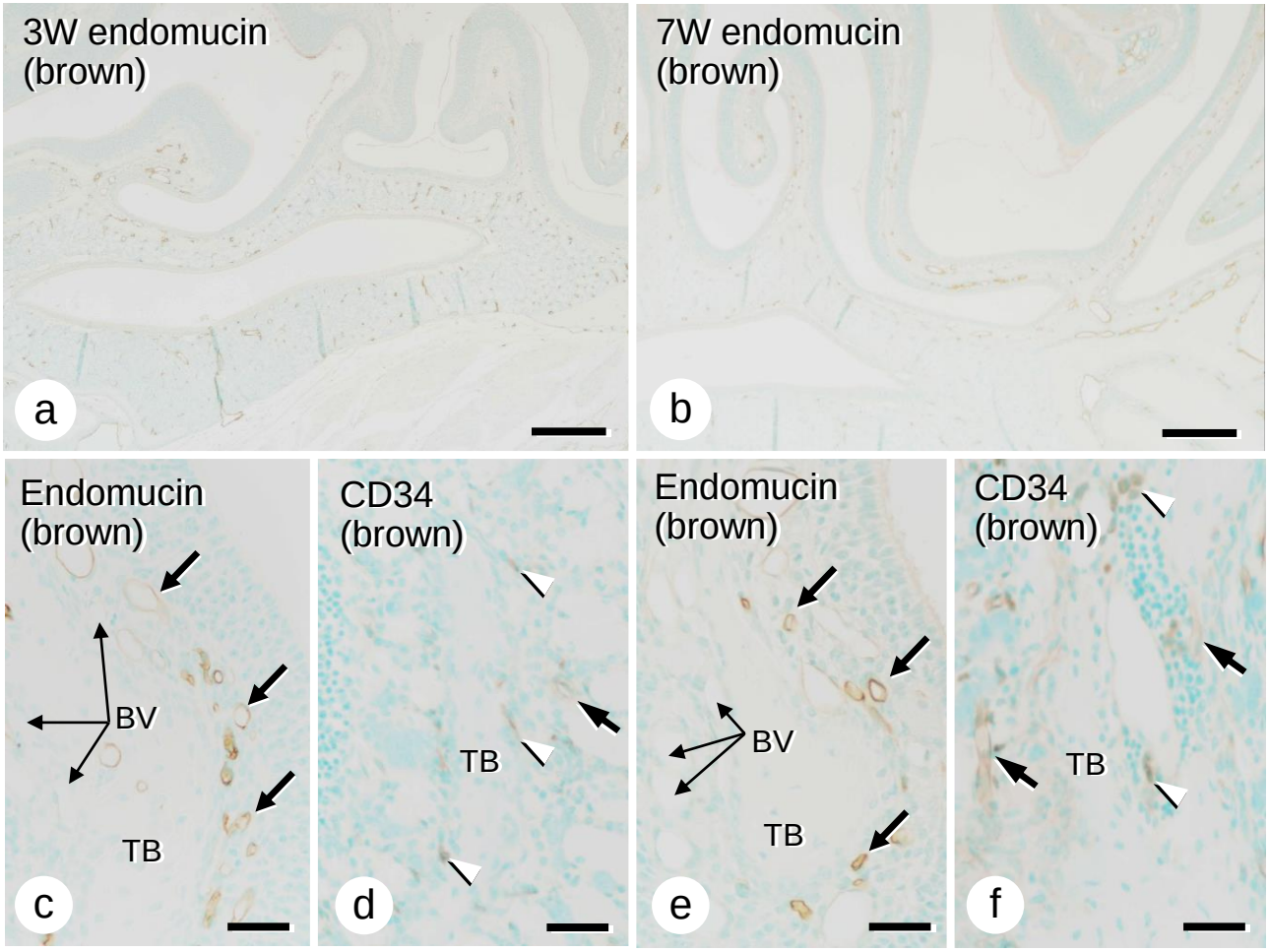
3W endomucin
(brown)
a
7W endomucin
(brown)
b
Endomucin
(brown)
BV
TB
c
CD34
(brown)
TB
d
Endomucin
(brown)
BV
TB
e
CD34
(brown)
TB
f

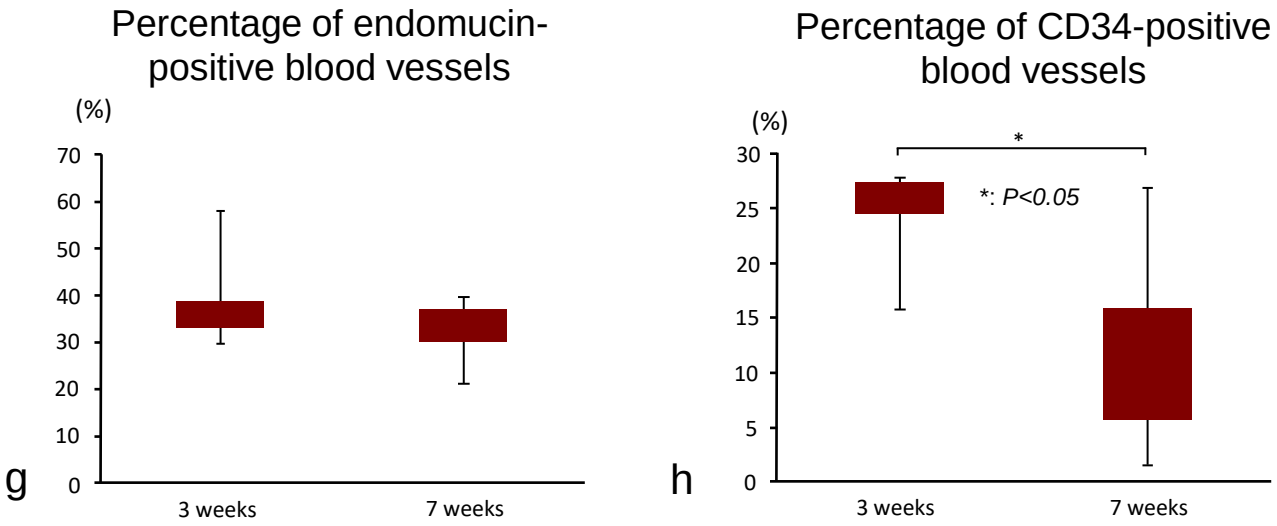
Percentage of endomucin-positive blood vessels
(%)
70
60
50
40
30
20
10
0
3 weeks
7 weeks
g
Percentage of CD34-positive blood vessels
(%)
30
25
20
15
10
5
0
*
*: P<0.05
3 weeks
7 weeks
h

Fig.2

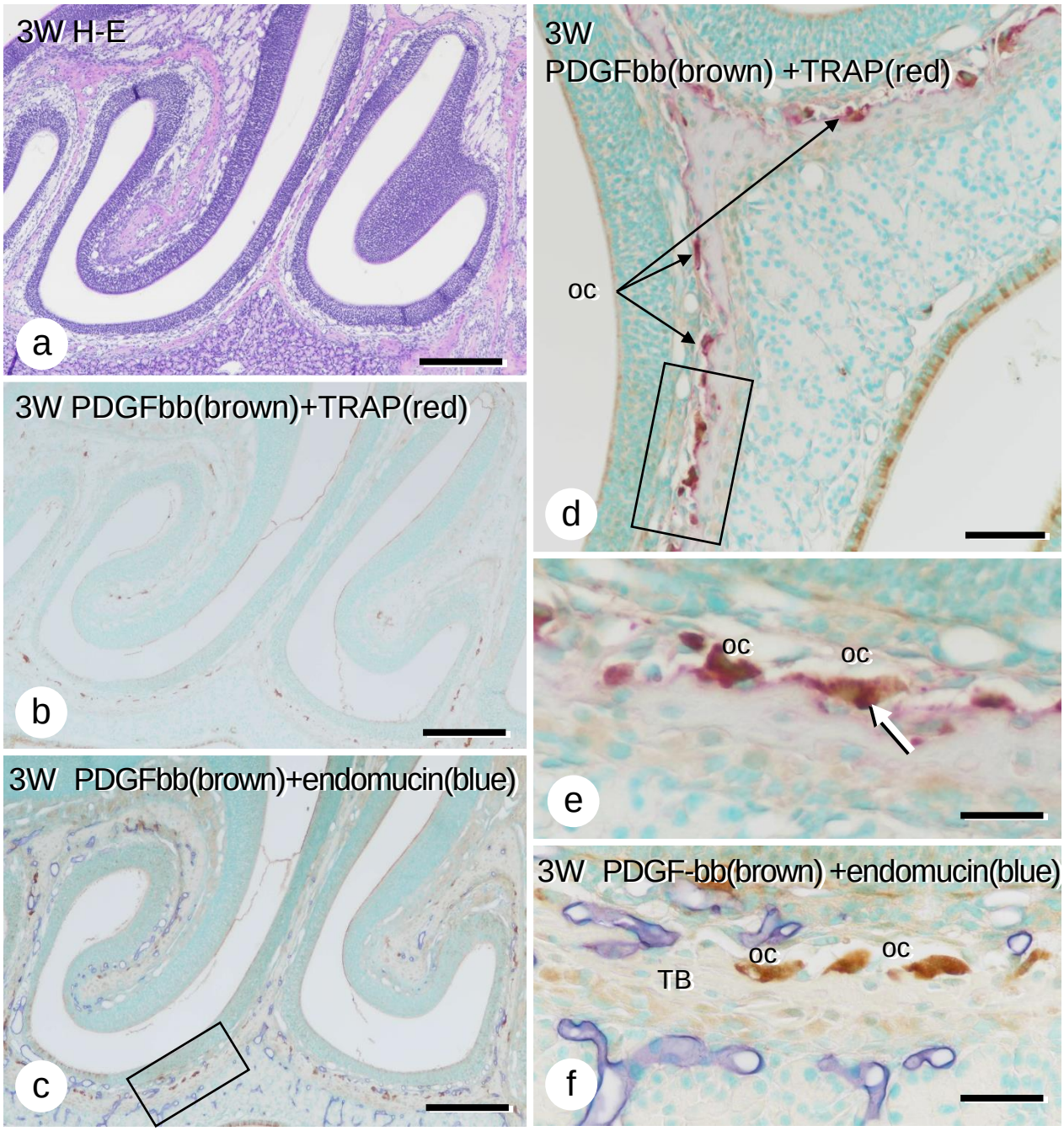
3W H-E
a
3W PDGFbb(brown)+TRAP(red)
b
3W PDGFbb(brown)+endomucin(blue)
c
3W
PDGFbb(brown) +TRAP(red)
oc
d
oc
oc
e
3W PDGF-bb(brown) +endomucin(blue)
oc
oc
TB
f

Fig.3

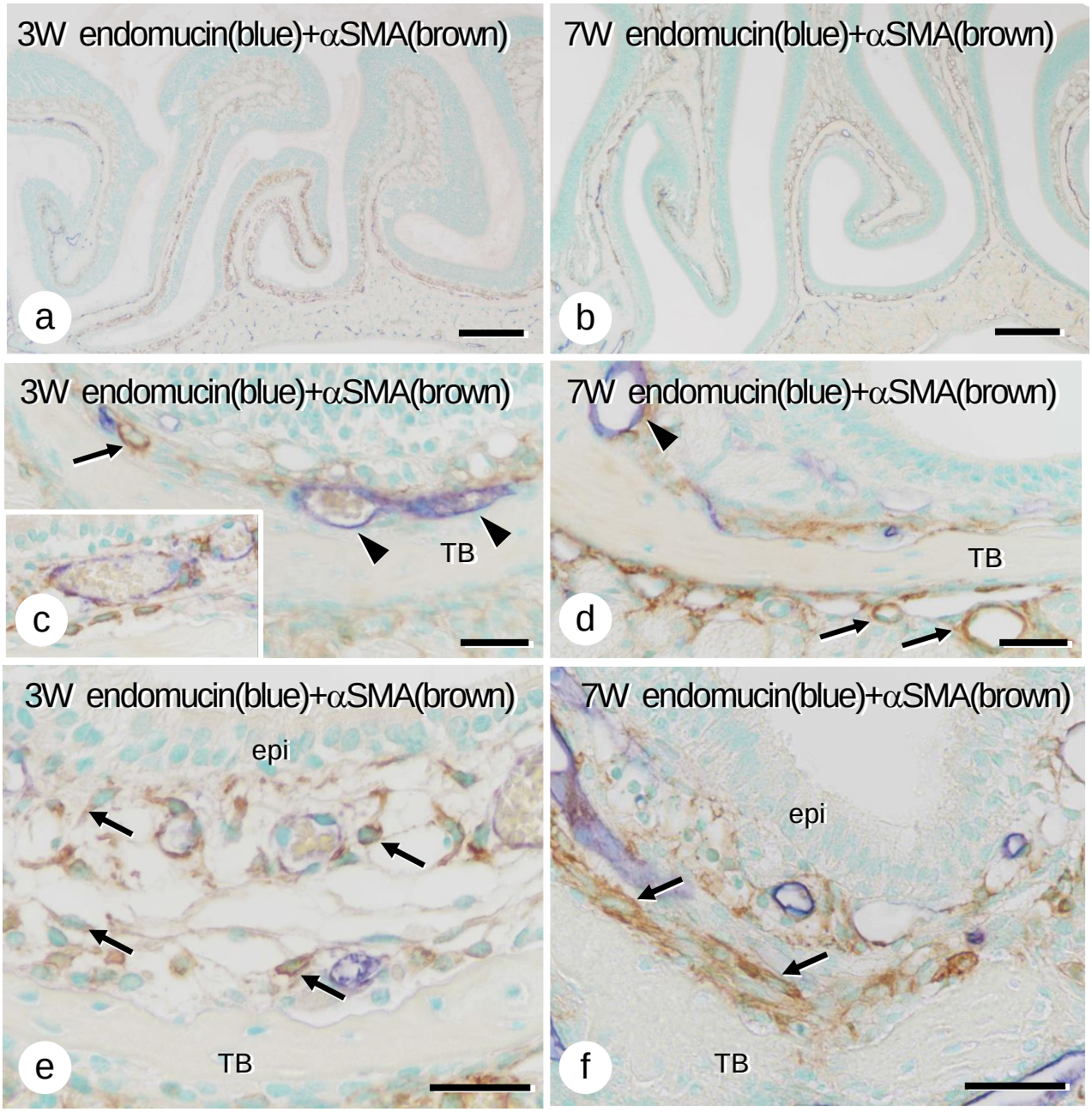
3W endomucin(blue)+αSMA(brown)
a
7W endomucin(blue)+αSMA(brown)
b
3W endomucin(blue)+αSMA(brown)
TB
c
7W endomucin(blue)+αSMA(brown)
TB
d
3W endomucin(blue)+αSMA(brown)
epi
TB
e
7W endomucin(blue)+αSMA(brown)
epi
TB
f

Fig.4

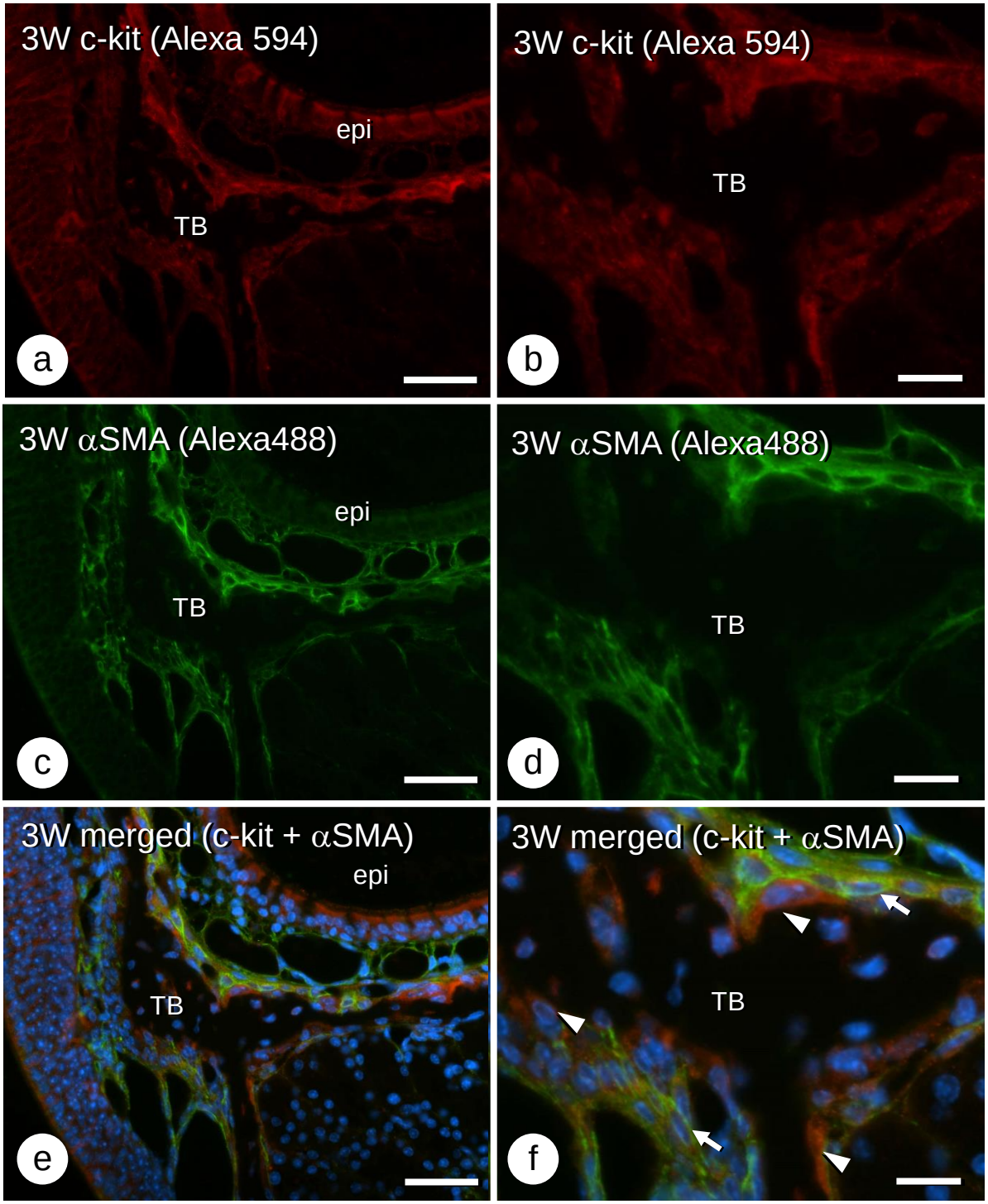
3W c-kit (Alexa 594)
epi
TB
a
3W c-kit (Alexa 594)
TB
b
3W αSMA (Alexa488)
epi
TB
c
3W αSMA (Alexa488)
TB
d
3W merged (c-kit + αSMA)
epi
TB
e
3W merged (c-kit + αSMA)
TB
f

Fig.5

Figure Legends

Figure 1

Histology of the nasal conchae of mice at 3 and 7 weeks of age

Panels **a** and **b** show images at lower magnification of the nasal conchae of 3-week (3W)-old **(a)** and 7-week (7W)-old mice **(b)**. The trabecular bone (TB) of the nasal conchae at 3 weeks of age shows a woven bone profile **(c)**, while that of 7-week-old mice reveals a relatively matured histology **(d)**. Panels **e** and **f** are highly magnified images of the boxed areas of panels **c** and **d**, respectively. In panels **e** and **f**, the lamina propria overlying the conchae bone includes many blood vessels (BV). epi: epithelium

Bars, **a** and **b**: 200μm, **c–f**: 40μm

Figure 2

Distribution of endomucin-immunoreactive blood vessels and CD34-positive cells in the nasal conchae

Panels **a** and **b** are the low power images of immunolocalization of endomucin-positive blood vessels (brown) in the nasal conchae of 3-week-old **(a)** and 7-week-old mice **(b)**. In the conchae at 3 weeks of age (**c**), some blood vessels display the brown-colored immunoreactivity of endomucin (black arrows), while other blood vessels show no endomucin-reactivity (BV with connected fine arrows). Similarly, at 7 weeks of age (**e**), some blood vessels showed endomucin-reactivity (brown colored blood vessels indicated by arrows), but the others demonstrated no immunoreactivity of endomucin (BV with connected fine arrows). Panels **d** and **f** demonstrate the immunolocalization of CD34-positive cells (brown color, white arrowheads) and small blood vessels (brown color, black arrows) in the nasal conchae of 3-week-old **(d)** and 7-week-old mice **(f)**. Panels **g** and **h** show statistical analyses by the Mann-Whitney U test on the percentages of endomucin-positive **(g)** and CD-34-positive blood vessels **(h)** in the nasal conchae of 3-week-old and 7-week-old mice. There was no significant difference in the percentage of endomucin-positive blood vessels both in 3-week-old and 7-week-old mice. Notice the significant difference between the percentages of CD34-positive blood vessels in 3-week-old and 7-week-old mice ($P<0.05$). TB: trabecular bone

Bars, **a** and **b**: 200μm, **c–f**: 20μm

Figure 3

Distribution of PDGFbb-positive/TRAP-reactive osteoclasts and endomucin-positive blood vessels in the nasal conchae

Panels **a–c** show images of the serial histological sections of the nasal conchae **(a)**, and double detection of PDGFbb (brown)/TRAP (red) **(b)** and PDGFbb (brown)/endomucin (blue) **(c)**. Notice the many PDGFbb-positive/TRAP-reactive osteoclasts (oc) located on one side of the conchae bone **(d)**. Panel **e** is a highly magnified image of the boxed area in panel **d**. TRAP-positive osteoclasts (oc) reveal brown-colored PDGFbb-positivity (white arrow, **e**). Endomucin-positive blood vessels (deep blue color) are seen not only on one side of the trabecular bone (TB) alongside the many TRAP-positive/PDGFbb-reactive osteoclasts (oc), but also on the other side **(f)**. Panel **f** is a highly magnified image of the boxed area in panel **c**.

Bars, a–c: 200μm, **d**: 50μm, **e, f**: 10μm

Figure 4

Distribution of αSMA-reactive cells in the nasal conchae

All panels of Figure 4 show double detection of endomucin-positive blood vessels (deep blue color) and αSMA-reactive cells (brown color) in the conchae of both 3-week-old **(a, c, e)** and 7-week-old **(b, d, f)** mice. In the region of the thin lamina propria **(c, d)**, endomucin-positive (blue color) blood vessels without αSMA-positive vascular smooth muscle cells (brown color) (black arrowheads in panels **c** and **d**) and endomucin-negative but αSMA-positive blood vessels (brown color, black arrows in panels **c** and **d**) are visible. Notice that endomucin-positive (deep blue)/αSMA-reactive (brown color) blood vessels are also observable (See the inset of panel **c**). In the thick layer of the lamina propria **(e, f)**, many fibroblastic cells positive for αSMA (brown color) can be seen in 3-week-old **(e)** and 7-week-old mice **(f)**.

Bars, a and **b**: 300μm, **c–f**: 20μm

Figure 5

Double immunofluorescence of c-kit and αSMA in the nasal conchae of 3-week-old mice

Panels **a–d** show c-kit **(a, b)** and αSMA **(c, d)** immunofluorescent images, respectively. Panels **e** and **f** are merged images of c-kit and αSMA immunofluorescent images observed at a lower **(e)** and higher **(f)** magnification. Notice that αSMA-positive cells (white arrows in panel **f**) can

be seen in close proximity of, but not overlapping with, c-kit-positive cells (white arrowheads in panel **f**). TB: trabecular bone, epi: epithelium

Bars, **a, c, e**: 30μm, **b, d, f**: 10μm